Proceedings of ASME Turbo Expo 2011
GT2011
June 6-10, 2011, Vancouver, British Columbia, Canada

GT2011-46747

DESIGN AND ANALYSIS OF A NEW ACCESSORY GEARBOX HOUSING FOR A GAS TURBINE ENGINE

Partha S. Das, Ph.D.
Mechanical Systems, Structures & Dynamics
Honeywell International, Inc.
111 S. 34th Street
Phoenix, AZ 85072, U.S.A.
Ph : (602) 231-3025
Fax : (602) 231-1313
E-mail : Partha.das@honeywell.com

ABSTRACT

Accessory Gearbox (AGB) Housing is one of the most critical components of a gas turbine engine that lies between the core engine & the aircraft. The function of the AGB Housing is to provide support for the gear drive assembly that transfers power from the engine to the engine accessories and to the power takeoff drive for the aircraft accessories. The housing also functions as an oil tight container and passageway for lubrication. In addition, the AGB housing provides mount points to attach engine/aircraft support accessories, including the engine mount points to the aircraft.

The complexity in predicting AGB housing behavior under the gear loading, engine loading and engine induced vibration is one of the main challenges of designing a new gearbox with minimum weight. To address these issues, the current paper presents for the first time the design-analysis of a new lightweight AGB housing for a turboshaft engine, based on the following three major requirements: i) gear bearing pads strength & stiffness capability, ii) AGB mount pads (for accessories and for engine) load carrying capability, and, iii) vibratory response (mainly high cycle fatigue (HCF) response) of the AGB housing. A 3-D Finite Element Analysis (FEA) model of the AGB housing was developed using the proposed initial design. Various design modifications, involving several interrelated, iterative steps, were then carried out by adjusting and modifying the housing wall thickness, placement & sizes of internal ribs and external gussets, including additional geometric modifications to satisfy the design objectives. The result is a robust, lightweight AGB housing design, eliminating the need for some of the required testing for the qualification of the new gearbox, indicating a significant cost savings. This paper also discusses in detail the methodology for the gear bearing pad strength/stiffness calculation, the FEA modeling techniques for the application of mount loads and gear bearing loads under operating & flight maneuver conditions, and, a methodology for addressing a combined HCF & LCF (Low Cycle Fatigue) response of the housing.

1. INTRODUCTION

Accurate structural design in the aircraft industry by fulfilling the design objectives and predicting its life well ahead of its field application has become a common requirement, because of the better understanding of the overall system as well as due to the advancement in the available various numerical tools. Increasing fuel costs have also encouraged more fuel efficient propulsion systems for the aircraft industry. Design requirements, such as low weight and high power capacity should be balanced with high life and low maintenance costs. Numerical/analytical tools predicting the life of a structure can be a valuable asset in the design of a gearbox or in the comparison of different gearbox designs.

McIntire & Wagner [1] and Godston & Kish [2] discussed arrangements for reduction gearboxes & the design requirements for the advanced prop-fan propulsion systems. Lewicki, et al [3] presented the life and reliability of the complete gearbox based on the lives and reliability of the bearings & gears only. Efficiency of aircraft gearboxes were also addressed by Anderson, et al [4] by modeling internal spur gear geometry and the effects of planetary motion. All these early studies discussed about gearboxes, based on gears & bearings only, without including the effect/impact of the AGB housing.

Inoue, et al [5, 6] proposed an optimum design method for a thin-plate structure which minimizes the vibration energy, and, applied it to the design of a gearbox housing for low vibration. These optimizations were attained by varying the plate thickness or changing the shape. The shape optimization is rather effective; however, the shape of the gearbox is prescribed in most of the cases. The redesign of the housing is, therefore, very difficult in such cases; instead, rib stiffening is frequently adopted, which is found to be the key to the design. Several studies have been reported on the rib layout design [7, 8], although the search for a perfect layout is not always easy. Since the search for the optimum layout is a time consuming task, a genetic algorithm [9] was used to minimize compliance design [10] and low vibration design [11] of the stiffened plate. Inoue, et al [12] discussed the optimum stiffener layout in a gearbox housing by placing stiffeners along the line from the point of excitation to a fixed point to lower vibration deflection of the faces with bearings only, however, did not discuss about the strength, stiffness of the housing on the misalignment of the gears or shafts.

Various factors affecting the gear mesh misalignment were discussed in details by Houser, et al [13], where the housing deflections was identified as one of the critical factors which may exceed those of the bearings. Therefore, reduction in housing deflections at the gear bearing pads in both in-plane & out-of-plane are critical in lowering the gear misalignment. In addition, having appropriate mount & accessory pads strength of an AGB housing with lower impact from vibratory responses (HCF & LCF) will lead to a successful design.

The objective of the work reported herein was to provide a complete design-analysis methodology for an AGB housing by addressing the following three major requirements, and, they are –

- i) Gear bearing pads strength & stiffness capability : Two new parameters, Shaft Misalignment (SM) and Shaft Angular Rotation (SAR), introduced to define in-plane & out-of-plane stiffness of the housing, respectively, and, then application of SM & SAR to define the rib positioning in the housing in order to reduce the misalignment of the gears,
- ii) AGB mount pads (for accessories & for engine) load carrying capability : Methodology for determining mount loads & accessory loads from maneuver load diagrams, FEA modeling details and iterative procedures for external/internal gussets positioning to address the strength of the mounts, and,
- iii) Vibratory response of the AGB housing : a complete new step by step analysis methodology to define HCF response, including a methodology for addressing a combined HCF & LCF responses of the housing.

2. ACCESSORY GEARBOX (AGB)

A cross-sectional view of a typical turboshaft engine, as shown in Fig. 1, shows also the cross-sectional view of an AGB, located at the front of the engine. The input rotors (GG & PT rotors), see Fig. 1, drive all the gears in the gearbox, which then provide power to drive all the accessories, including the output shaft. This generates significant amount of radial loadings on all the gear bearing pads of the case & cover of the AGB housing. Figures 2(a) & 2(b) shows three of the most critical gear bearing pad

.

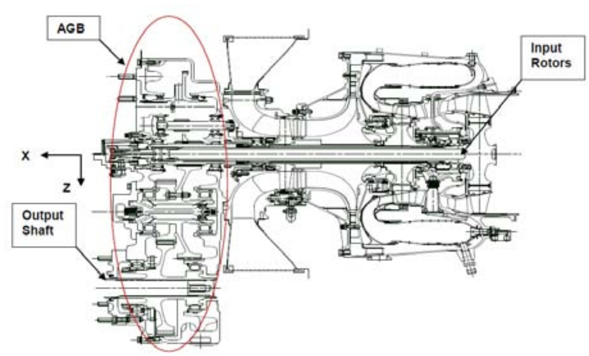

Figure 1 : Cross-Sectional View of a Typical Turboshaft Engine

locations (i.e. input, idler & output pads) in the current AGB housing, including the locations of various engine mount pads & the accessory pads.

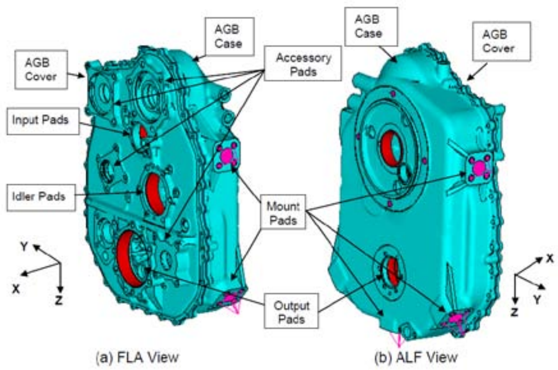

Figure 2 : AGB Housing with Three Critical Gear Bearing Pad Locations, Including Various Engine Mount and Accessory Pads

3. STRENGTH & STIFFNESS OF GEAR BEARING PADS

To calculate the strength & stiffness of a gear bearing pad, two new parameters, SM and SAR are introduced. The SM represents in-plane movement of the center of the bearing pad, and, SAR out-of-plane rotation of the bearing pad. The SM causes gear shafts to misalign, thus causing gears to mesh improperly, resulting in excessive gear wear and, consequently, low gear life. The SAR causes "cocking" of bearing that is mounted in each pad, may possibly contribute to misalignment of fwd and aft pads relative to each other as well. Lowering the SM & SAR of the gear bearing pads by properly positioning the internal ribs are one of the main objectives here.

The detailed analysis methodology for calculating SM & SAR are presented below :

Step 1: Identify 2N (where N is an even '+'ve integer), as shown in Fig. 3, equally spaced points (nodes) around the circumference of the bearing bore of each gear bearing pad, such that points 1 & (N+1) align with the vertical (Z) axis and points (N/2+1) & (3N/2+1) align with the lateral (Y) axis.

Step 2: Find the diameter (d) of bearing bore of each pad.

Step 3: Create a local Cartesian coordinate system (e.g. csys,100 in Fig. 3) at the center of each pad, where local Cartesian coordinate directions are parallel to the global Cartesian directions (csys, 0).

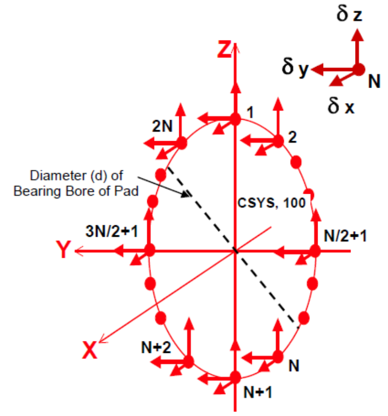

Figure 3 : Location of 2N Points in a Typical Gear Bearing Pad

Step 4: Read the analysis result file (i.e. results from the gear bearing pads strength & stiffness analysis), activate local Cartesian coordinate system created in Step 3 and get axial displacements (i.e. $\delta x1$, $\delta x2$, … $\delta x2N$), lateral displacements (i.e. $\delta y1$, $\delta y2$, … $\delta y2N$), and, vertical displacements (i.e. $\delta z1$, $\delta z2$, … $\delta z2N$) for all 2N points identified in Step 1.

Step 5: Calculate the average lateral (Y-axis) displacement (δy) of the centerline of the bearing pad by the following equation :

$$\delta y = (\delta y1 + \delta y2 + \ldots\ldots + \delta y2N)/2N \qquad (1)$$

Step 6: Calculate the average vertical (Z-axis) displacement (δz) of the centerline of the bearing pad by the following equation :

$$\delta z = (\delta z1 + \delta z2 + \ldots\ldots + \delta z2N)/2N \qquad (2)$$

Step 7: Determine the center of the bearing pad displacement, δyz, and, direction, θyz, relative to the vertical (Z) axis, see Figs. 4(a) & 4(b), using the following equation:

$$\delta yz = \sqrt{\delta y^2 + \delta z^2} \qquad (3)$$
$$\theta yz = \tan^{-1}(\delta y / \delta z)$$

Step 8: Determine the gear Shaft Misalignment (SM) using the following equation:

$$SM = \sqrt{\left((\delta y_{FWD} - \delta y_{AFT})^2 + (\delta z_{FWD} - \delta z_{AFT})^2\right)} / Lx \qquad (4)$$

Where, δy_{FWD} & δz_{FWD} are average lateral & vertical displacements of the forward pad (i.e.

pad in AGB cover), respectively, δy_{AFT} & δz_{AFT} average lateral & vertical displacements of the aft pad (i.e. pad in AGB case), respectively, and, Lx is the distance between the forward & aft gear bearing pads (see Figs. 4(a) & 4(b)).

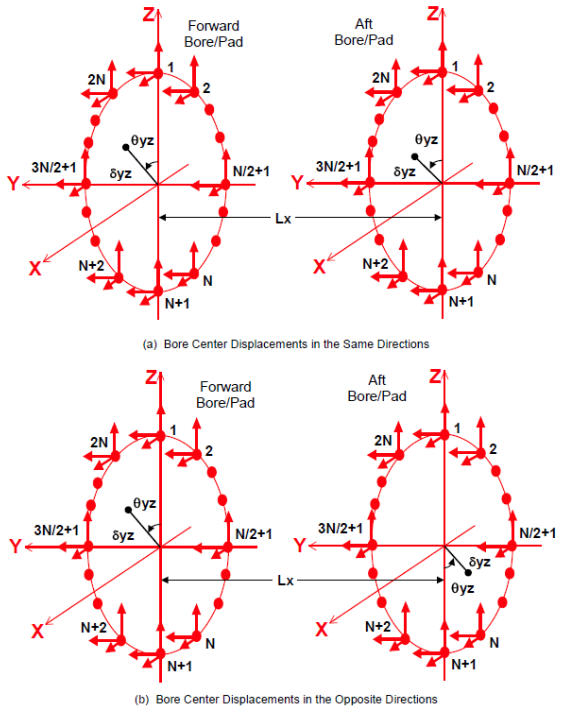

Figure 4 : Gear Bearing Pads In-Plane Displacements for SM

Step 9: Calculate the gear bearing pad out-of-plane rotation, see Fig. 5, for each pair of opposing points (i.e. 1:N+1, 2:N+2, ….., and, N:2N, see Fig. 3), as follows :

$$\Theta_{1:N+1} = \{(\delta_{x1} - \delta_{x(N+1)})/d\}$$
$$\Theta_{2:N+2} = \{(\delta_{x2} - \delta_{x(N+2)})/d\}$$
$$\ldots\ldots\ldots\ldots\ldots\ldots\ldots\ldots \quad (5)$$
$$\Theta_{N:2N} = \{(\delta_{x(N)} - \delta_{x(2N)})/d\}$$

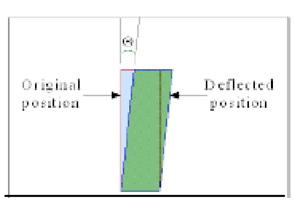

Figure 5 : Gear Bearing Pad Out-of-Plane Rotation for SAR

The highest value among $\Theta_{1:N+1}$, $\Theta_{2:N+2}$, ……, and, $\Theta_{N:2N}$, obtained from Eq. 5, determines the gear Shaft Angular Rotation (SAR) for each bearing pad.

3.1 Three Dimensional (3-D) FEA Modeling

The full scale, 3-D FEA model for the accessory gearbox housing, was generated using the FEA software ANSYS [14]. The main engine section, considered in the present study, is also included in the model, and, was represented as a cylindrical structure, attached to the AGB housing, to simulate the appropriate boundary conditions for the AGB housing analyses. The arbitrary quadrilateral 10-noded 3-D structural solid element, SOLID92 [15], has been adopted for the gearbox, because of its compatible displacement shapes & well suited to model irregular geometries, including the large deformation and large strain capabilities. The bolt hole locations of the AGB cover & case were coupled in local radial, hoop & axial directions, while the bolt hole edges between the AGB case & the engine cylinder were coupled in local axial & hoop directions, and, pilot surfaces between them in the local radial direction. A special 3-D 8-noded contact element CONTA174 [15] was used in combination with the 3-D target surface element TARGE170 [15] to define the contact surfaces in between AGB case & cover as well as between AGB case & engine cylinder.

A typical discretized 3-D FEA model of the AGB housing, including the engine cylinder, is shown in Fig. 6. High density meshing has been used throughout the gearbox model to capture the deformation & stress distribution more accurately. The FEA model in Fig. 6 contains a total of ~300,000 elements, and ~570,000 nodes.

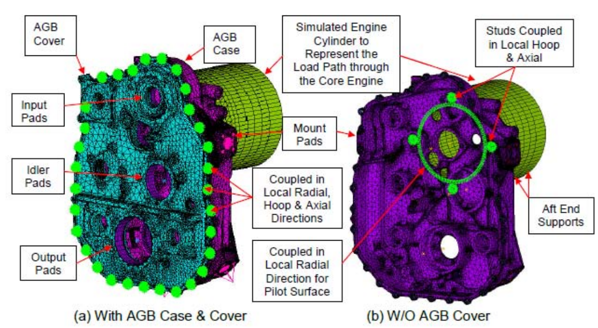

Figure 6 : A Discretized 3-D FEA Model of the AGB Housing, Including the Engine Cylinder

3.2 Analyses and Results

Figures 7(a) & 7(b) show the gear bearing loads (P_i & θ_i) on the AGB cover & case bearing pads, respectively, under the maximum operating conditions. For a fixed set of gears, it is to be noted that the resultant of the gear loading directions (θ_i) on the bearing pads, where the actual loads are parabolically distributed over the gear bearing pads, as shown in Figs. 7(a) & 7(b), remain same. It is also to be noted that the resultant load (P_i) may vary depending on the speed of the shaft/gears and the output power, however, the loading directions (θ_i) on the bearing pads for a particular set of gears remain constant.

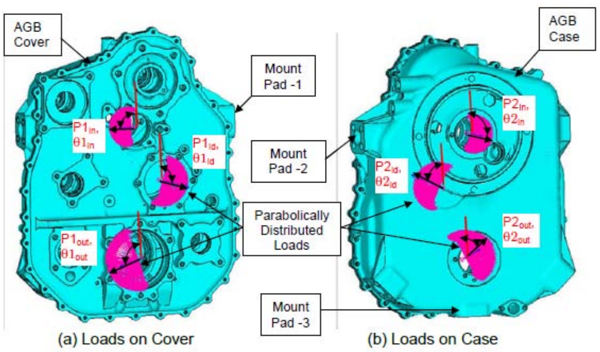

Figure 7 : Gear Bearing Loads at Max Operating Conditions

For the gear bearing pads strength & stiffness analysis, Mount Pad-1 & Mount Pad-2 (as shown in Fig. 7) were fixed in all directions, whereas Mount Pad-3 were fixed only in axial (i.e. X) & lateral (i.e. Y) directions (see Fig. 2) to simulate the engine forward end support. For the aft end support, two locations at the aft end of the engine cylinder, as shown in Fig. 6, were fixed in axial (i.e. X) & lateral (i.e. Y) directions. Analyses were carried out by rearranging the AGB housing internal ribs in order to minimize the SM & SAR under the max operating loading conditions. Examples of some of the ribs addition & removal are shown in Fig. 8.

Tables 1 & 2 show the SM & SAR for the input, idler & output pads, respectively, which were calculated from the FEA results using the methodology presented earlier. Eight opposite nodes were used to determine the SM & SAR values for each pad, see the corresponding figures beside the Tables 1 & 2. The maximum SM & SAR values, obtained from Tables 1 & 2, respectively, were then compared with the allowable limits of SM & SAR to determine whether the rib definitions are acceptable or not.

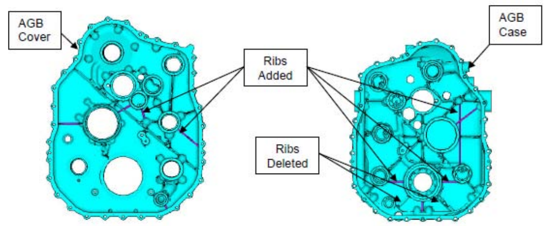

Figure 8 : Typical Example of Addition & Removal of AGB Housing Internal Ribs

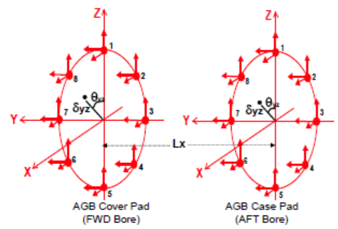

Gear Shaft	Shaft Misalignment (in/in)
Input	SM_{Input}
Idler	SM_{Idler}
Output	SM_{Output}

Table 1 : SM of Three Critical Locations of AGB Housing

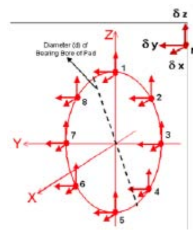

Gear Shaft	Shaft Angular Rotation (in/in)	
	Opposite Nodes	New GB
FWD Input	θ4-8	$SAR_{FWD\text{-}Input}$
FWD Idler	θ3-7	$SAR_{FWD\text{-}Idler}$
FWD	θ4-8	$SAR_{FWD\text{-}Output}$
AFT Input	θ1-5	$SAR_{AFT\text{-}Input}$
AFT Idler	θ2-6	$SAR_{AFT\text{-}Idler}$
AFT Output	θ3-7	$SAR_{AFT\text{-}Output}$

Table 2 : SAR of Six Pads in Three Critical Locations of AGB Housing

4. LOAD CARRYING CAPABILITIES OF THE AGB MOUNT & ACCESSORY PADS

This section presents the analysis methodology for the AGB mount & accessory pads load carrying capabilities under various flight maneuver conditions, as shown in Fig. 9. This section also presents an iterative technique to improve the pads capabilities in order to meet the design requirement.

A schematic diagram of the engine AGB mount pad geometry is shown in Fig. 10. Each mount pad is configured with four threaded holes with inserts to withstand the pullout and torque loads, and, the pad center has a close tolerance hole to accommodate a shear plug from the aircraft attachment bracket to react transverse shear loads. For typical accessory pads, see Fig. 2.

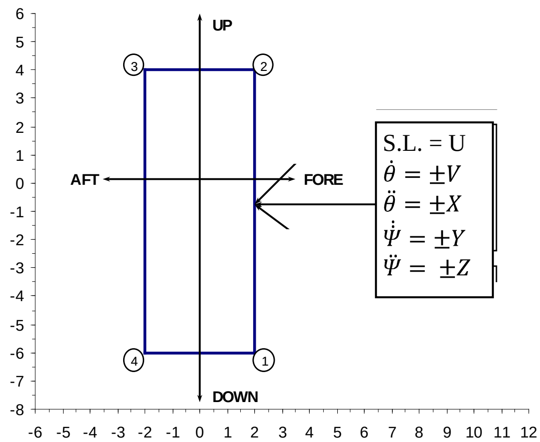

Figure 9 : A Typical Flight Maneuver and Inertia Load Diagram

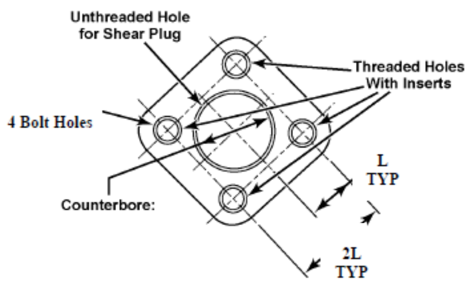

Figure 10 : Engine AGB Mount Pad Schematic

4.1 3-D FEA Model for AGB Mount & Accessory Pads Analysis

The same FEA model, as shown in Fig. 6, was used for the current analysis. In addition, a special beam modeling technique, as described below, was used for the application of the maneuver loads from airframe to the engine forward mount pads that are integral to the AGB housing. Details of the beam modeling at one of the AGB mount pads are shown in Fig. 11. The steps for the beam modeling technique are as follows :

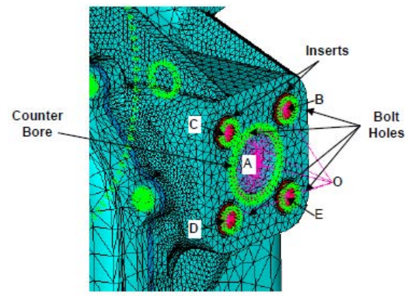

Figure 11 : Beam Modeling at AGB Mount Pads

<u>Step 1</u> :Create a central node at each insert hole location, such as node A, B, C, D and E, where A represents the center node of the counter bore, and, B-E the center nodes of the 4 threaded bolt holes.

<u>Step 2</u> :Create another node at O, where O is the node where all the maneuver loads are applied and OA is a typical industry standard mount pad surface distance offset of 1.5 inches, perpendicular to the mount pad face.

<u>Step 3</u> :Generate a set of nodes at the counter bore hole edge, by copying the nodes at the same location, connect these copied nodes with the central node A using rigid beam elements, and, then couple these copied nodes with their corresponding nodes on the counter bore hole edge in the local radial and hoop directions, in order to allow only movement in the axial (i.e. perpendicular to the mount pad) direction to simulate the shear plug behavior.

<u>Step 4</u> :Generate separate set of nodes at all the insert hole inner edges (i.e. a total of 4 sets), by copying the nodes at the same location, connect these copied nodes with their respective central nodes, such as, nodes B, C, D & E, using rigid beam elements, and, then couple these copied nodes with their corresponding nodes on the inner edge of insert holes only in the axial (i.e. perpendicular to the mount pad) direction locally, since these nodes only take the loads in the axial direction from the bolt loads.

<u>Step 5</u> : Generate 5 more rigid beams connecting A, B, C, D and E with O, where all the maneuver loads, applied at O, can be transferred properly to the AGB mount pads.

For accessory pads, since the accessories were not the focus of the study, they were represented as a mass element, MASS21 [15] at their corresponding center of gravity (CG) locations. The mass elements were then connected to the accessory pads or to their supporting brackets that are attached to the AGB housing using the similar beam modeling technique, as for mount pads. Figure 12 shows a typical 3-D FEA model with external accessories, represented as mass elements, and, attached to the AGB housing directly or through a supporting bracket.

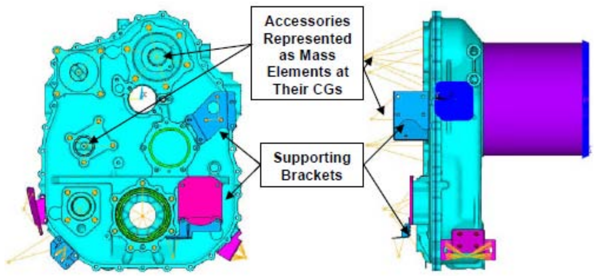

Figure 12 : 3-D FEA model of the AGB Housing with External Accessories

4.2 Engine Mount Pad & Accessory Pads Loads

The mount loads for all corner points of the flight maneuver envelop, as shown in Fig. 9, were determined using the Honeywell's engine mount load program. The program, in addition to inputs from flight maneuver diagram, uses the following information, such as, mount locations, engine total weight & CG, engine mass moment of inertia, GG & PT rotor speeds, output torque, engine thrust, etc. for calculation of the mount loads under various flight maneuver conditions. For accessory loads, the maneuver diagram, as shown in Fig. 9, were first updated due to the differences in CG locations between the AGB & engine CGs. The overall 'G' loadings at the engine CG (see Fig. 9) were modified by additional 'G' loadings using the following equations :

$$G_{Ang\_Accl} = \Delta S * \ddot{\beta} \qquad (6)$$

$$G_{Ang\_Vel} = \Delta S * \dot{\beta}^2 \qquad (7)$$

where, G_{Ang_Accl} & G_{Ang_Vel} are 'G' loadings due to angular acceleration & velocity, respectively, $\triangle S$ is the CG offset distance, and, $\ddot{\beta}$ & $\dot{\beta}$ are angular acceleration & velocity, respectively. Following the updates, the accessory loads were determined by simply multiplying the updated maneuver 'G' loadings with their corresponding weights.

4.3 Analyses & Results

The FEA models, as shown in Figs. 6, 11 & 12, were used to capture the detailed stress distributions in the vicinity of the AGB mount & accessory pads. Mount loads were applied simultaneously at the mount pads and reacted through the bolt-on cylinder at the aft side of the gearbox housing. From an analysis model perspective, the cylinder is equivalent to the engine case. The length of the cylinder represents the distance of the diffuser/combustor plenum flange location from the engine mounts, as well as, the engine aft mount locations. It is to be noted that the mount pad capabilities related to bolt preloads, inserts, and shear plug, and the various mount pad failure modes, such as, mount pullout, tensile tear out, pad bending moment, etc. were verified with the standard equations, for which FEA solutions were not used.

Iterative analyses were carried out by adding/modifying external & internal gussets at the various mount pads in order to meet the design requirement. Mount Pad-2, as an example, has been selected here to show the impact of gusset's orientation & thickness on the pad capabilities.

The external & internal views of the initial geometry of the Mount Pad-2 are shown in Figs. 13(a) & 13(b), respectively, whereas, Fig. 13(c) shows the corresponding max stress distribution in the pad under one of the critical maneuver load cases. Higher than allowable stresses was observed in Mount Pad-2, as indicated in Fig. 13(c). The external gussets in vertical direction, as shown in Fig. 14(a), were added with varying thickness as a first attempt to increase the pad's strength & stiffness capabilities. A nominal improvement was noticed for the Mount Pad-2, as indicated by its displacement & stress plots (see Figs. 14(b), 14(c) & 14(d)). However, a significant improvement in the pad's strength capability was noticed, as two axial direction external gussets & several internal gussets, as shown in Figs. 15(a) & 15(b), respectively, were added. Similar results were obtained with 2 vertical & 2 diagonal external gussets (see Figs. 16(a) & 16(b)), instead of 4 vertical & 2 axial gussets (Fig. 14(a)), and was selected as the final configuration for the Mount Pad-2 due to lower number of external gussets. Similar iterative methodology was also followed for other mount pads. For additional weight savings, it is to be noted that some of the materials from the mount pads can also be scalloped out, as indicated in Fig. 16(b).

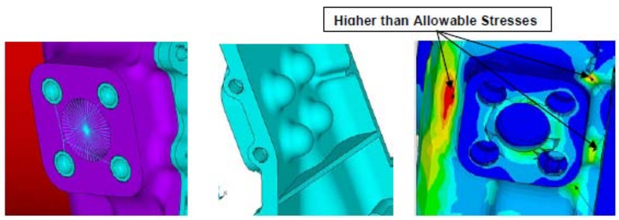

(a) External View (b) Internal View (c) Stress Distribution

Figure 13 : Initial geometry of Mount Pad-2, Including Max Stress Distribution

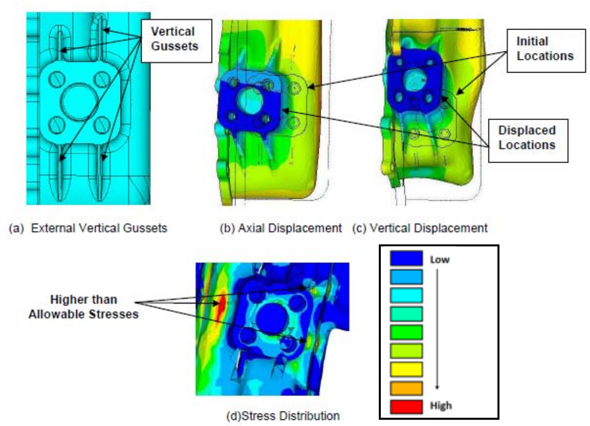

Figure 14 : Effect of Vertical Gussets on Mount Pad-2

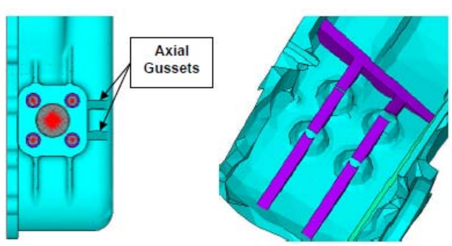

(a) External Vertical & Axial Gussets (b) Internal Gussets

Figure 15 : Additional External & Internal Gussets in Mount Pad-2

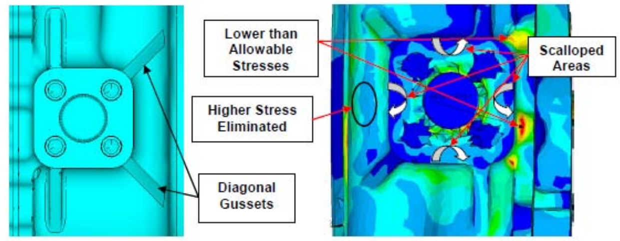

(a) External Vertical & Diagonal Gussets (b) Stress Distribution

Figure 16 : Final External Gusset Locations in Mount Pad-2

5. VIBRATORY RESPONSE OF THE AGB HOUSING

The 3-D FEA model, as shown in Fig. 11, was also used to investigate the vibratory response of the AGB housing. The AGB mount pads & aft end of the engine cylinder were used to apply the appropriate boundary conditions for the current analysis. Das [16] in his earlier work had discussed in detail a combined experimental-computational technique for the vibration characteristics of the externals and their impact on the AGB housing. However, instead of a combined technique, the current work, as described below, presents a new computational methodology to determine the vibration characteristics of the AGB housing in order to help with the design process. Here are the steps for the current methodology :

Step 1 : Perform a modal analysis to identify the resonant frequencies and the corresponding mode shapes of the housing.

Step 2 : Perform Harmonic Response Analysis (HRA) in three mutually perpendicular directions independently, under the excitation force amplitude of '1G' acceleration, and, over the frequency range of interest.

Step 3 : Determine the maximum stresses of the AGB housing at each resonant frequency (for all 3 directions), which are due to '1G' acceleration load.

Step 4 : Identify the max stress of the AGB housing from Step 3 results (within the engine operating frequency range). Study/determine the impact of 'damping factor' on the variation of max stress of the AGB housing, since the exact value of the damping is unknown.

Step 5 : Determine the equivalent 'G' loading, corresponding to the HCF endurance strength of the AGB housing, based on the results from Step 4. Therefore, higher the value of 'G' loading, the lower is the possibility of having any concern with the HCF live of the AGB housing.

Step 6 : Superimpose the HCF results from Step 5 with the stress distribution in the housing, obtained from the analysis under gear bearing loads that defines the LCF life of the housing, to determine a combined life under the HCF & LCF responses.

Since the exact excitation force due to engine vibration is not known, the current proposed methodology will help to identify & if required, to minimize the potential risk of failure from the HCF response by improving the design of the housing. It is to be noted that the proposed methodology for the HCF response is currently being applied for the design of a new AGB housing. Detail analysis results and validation of the current methodology will be presented in the future work.

In summary, designing of a new lightweight AGB housing based on the three major requirements, as described in Sections 3-5, indicate a very robust design, and, therefore, has the potential of eliminating some of the required tests, such as, static load test, vibe test, etc. for the qualification of the new AGB housing, which can save a significant cost for qualifying a new AGB housing.

6. CONCLUSIONS

This paper presents a detailed methodology to analyze and design a new AGB housing based on three major requirements. They are :

a) Calculation of SM & SAR of the gear bearing pads and the placement of ribs to minimize the SM & SAR to reduce the gear wear for longer gear life,
b) The calculation of engine mount loads & AGB accessory loads, the FEA modeling technique for their applications, and, addition/modification of internal & external gussets, thickness variation, etc. at the mount & accessory pads to meet the pads strength, and,
c) Vibration analysis methodology to address the combined HCF & LCF lives of the housing.

Desired results from the above three sets of analyses lead to a robust design for a new lightweight AGB housing, and, therefore, has the potential of eliminating some of the qualification tests for a significant cost savings.

ACKNOWLEDGEMENTS

The author wishes to acknowledge MSSD Department, as well as, Honeywell Management with great appreciation for their support of this study and for permitting the publication of this paper. The author would also like to thank HTS-India for their help with FEA work.

NOMENCLATURE

AGB	Accessory Gearbox
AFT	Aft (i.e. AGB Case)
FWD	Forward (i.e. AGB Cover)
CG	Center of Gravity
HCF	High Cycle Fatigue
LCF	Low Cycle Fatigue
G	Acceleration, in/sec^2
GG	Gas Generator
PT	Power Turbine
N	An Even '+'ve Integer
SM	Shaft Misalignment
SAR	Shaft Angular Rotation
L_x	Distance between Fwd & Aft Gear Bearing Pads
G_{Ang_Accl}	'G' loadings due to Angular Acceleration
G_{Ang_Vel}	'G' loadings due to Angular Velocity
S.L.	Side Load
d	Diameter of the Gear Bearing Pad
δ_x	Axial (i.e. X-direction) Displacement
δ_y	Lateral (i.e. Y-direction) Displacement
δ_z	Vertical (i.e. Z-direction) Displacement
δ_{yz}	Center of the Bearing Pad Displacement
θ_{yz}	Center of the Bearing Pad Displaced Direction
$\Theta_{P:Q}$	Out-of-plane Rotation of a Gear Bearing Pad (Between Nodes P & Q)
$\dot{\theta}, \ddot{\theta}$	Pitching Velocity (rad/sec) & Acceleration (rad/sec^2)
$\dot{\Psi}, \ddot{\Psi}$	Yawing Velocity (rad/sec) & Acceleration (rad/sec^2)
$\triangle$S	CG Offset Distance

REFERENCES

1. McIntire, W. L., and Wagner, D. A., 1982, "Next Generation Turboprop Gearboxes," ASME Paper No. 82-GT-236.
2. Godston, J., and Kish, J., 1982, "Selecting the Best Reduction Gear Concept for Prop-Fan Propulsion Systems," AIAA Paper 82-1124.
3. Lewicki, D. J., Black, J. D., Savage, M., and, Coy, J.J., 1986, "Fatigue Life Analysis of a Turboprop Reduction Gearbox," Journal of Mechanisms, Transmissions, and, Automation in Design, Vol. 108, pp. 255-262.
4. Anderson, N. E., Loewenthal, S. H., and, Black, J. D., 1986, "An Analytical Method to Predict Efficiency of Aircraft Gearboxes", Transactions of the ASME, Vol. 108, pp. 424-432.
5. Inoue, K., Townsend, D. P., and Coy, J. J., 1993, ''Optimum Design of a Gearbox for Low Vibration,'' ASME J. Mech. Des., 115(4), pp. 1002–1007.
6. Inoue, K., Yasunami, M., and Kato, M., 1999, ''Shape Optimization of Gearbox Housing for Low Vibration,'' Proceedings of 4th World Congress on Gearing and Power Transmission, **3**, MCI, pp. 2053–2064.
7. Cheng, K. T., 1988, ''On Non-Smoothness in Optimal Design of Solid, Elastic Plates,'' Int. J. Solids Struct., Vol. 17, pp. 795–810.
8. Yamazaki, K., and Kobayashi, A., 1988, ''Optimum Compliance Design of Stiffener Layout of Thin Plate,'' Trans. Jpn. Soc. Mech. Eng., Ser. A, 54-A, pp. 1165–1171.
9. Goldberg, D. E., 1989, "Genetic Algorithms in Search, Optimization and Machine Learning", Addison-Wesley Publishing Co., Inc.
10. Inoue, K., Fueki, H., Ohmachi, T., and Kato, M., 1995, ''An Application of Genetic Algorithms to Design of Stiffened Plates,'' Proceedings of 10th International Conference on Engineering Design, 4, WDK, pp. 1369–1377.
11. Inoue, K., Yamanaka, M., and Kihara, M., 1999, ''Acquisition and Evaluation of Knowledge on the Design of Stiffener Layout,'' Proceedings of 12th International Conference on Engineering Design, 3, WDK, pp. 1629–1634.
12. Inoue, K., Yamanaka, M., and Kihara, M., 2002, "Optimum Stiffener Layout for the Reduction of Vibration and Noise of Gearbox Housing", Transactions of the ASME, Vol. 124, pp. 518-523.
13. Houser, D. R., Harianto, J., and, Talbot, D., 2006, "Gear Mesh Misalignment", Gear Solutions.
14. ANSYS User's Manuals, Release 11.0, 2007.
15. ANSYS Elements Reference, Release 11.0, 2007.
16. Das, P. S., 2009, "A Combined Experimental-Computational Technique for the Vibration Characteristics of the Externals in Gas Turbine Engines", Proceedings of the 2009 ISABE Conference, Paper No. 2009_1119.